Journal of Alloys and Compounds 500 (2010) L1–L5

Contents lists available at ScienceDirect

Journal of Alloys and Compounds

journal homepage: www.elsevier.com/locate/jallcom

Letter

Synthesis of single-crystal $Ba_{1-x}Sr_xTiO_3$ ($x = 0–1$) dendrites via a simple hydrothermal method

Linlin Yang[a], Yonggang Wang[a,*], Yujiang Wang[a], Xiaofeng Wang[a], Xianjun Guo[a], Gaorong Han[b]

[a] Department of Materials Science and Engineering, Luoyang Institute of Science and Technology, Luoyang 471023, PR China
[b] State Key Laboratory of Silicon Materials, Department of Materials Science and Engineering, Zhejiang University, Hangzhou 310027, PR China

ARTICLE INFO

Article history:
Received 16 February 2010
Received in revised form 5 March 2010
Accepted 8 March 2010
Available online 2 April 2010

Keyword:
Nanostructured materials

ABSTRACT

In this paper, we report a simple hydrothermal method to synthesize barium strontium titanate ($Ba_{1-x}Sr_xTiO_3$, $x = 0–1$) dendrites without any templates. The obtained products were characterized by X-ray diffraction (XRD), transmission electron microscopy (TEM), electron diffraction (ED), and energy-dispersive X-ray spectroscopy (EDX), respectively. All the samples were identified as cubic perovskite phase by XRD and the obtained $Ba_{1-x}Sr_xTiO_3$ ($x = 0–1$) dendrites were single-crystal. The formation process of $Ba_{1-x}Sr_xTiO_3$ dendritic structures was also investigated. It is rational to expect that dendritic structures of other perovskite oxides may also be synthesized by this simple method.

1. Introduction

Nanostructures have received growing interest not only for their fundamental scientific significance but also for the many technological applications that derive from their peculiar and fascinating properties, superior to the corresponding bulk counterparts [1,2]. Especially, considerable attention has been focused on dendritic structures, which can be applied in photovoltaics and multifunctional nanoelectronics due to the large surface areas and continuous networks [3,4]. Up to now, a variety of dendritic crystals such as metal [5–7], metal oxide [8,9], and chalcogenide [10] have been successfully obtained. Barium strontium titanate ($Ba_{1-x}Sr_xTiO_3$) is an important ferroelectric and capacitor material [11,12]. $Ba_{1-x}Sr_xTiO_3$ nanopowders, star-shaped powders, brain-like shaped powders, and nanocubes have been successfully prepared [13–19]. Various techniques have been developed to synthesize $Ba_{1-x}Sr_xTiO_3$, such as co-precipitation procedure [13], flame spray pyrolysis [14], solution method [16], citric acid gel route [17], solvothermal method [19], and hydrothermal process [20]. A disadvantage in the hydrothermal preparation of BSTO is the control of stoichiometry and phase purity [20]. However, hydrothermal process is a facile, mild, and effective method for creating novel architectures or hierarchical structures based on nanocrystals [21]. For example, nanocrystals with different morphologies, such as $BaTi_2O_5$ nanobelts [22], $TbMn_2O_5$ nanorods [23], $CdWO_4$ nanorods [24], PbS dendritic nanostructures [10], and star-like MnO_2 crystals [8], have been synthesized by facile hydrothermal process. In the present paper, we report the preparation of $Ba_{1-x}Sr_xTiO_3$ ($x = 0–1$) dendrites by a simple hydrothermal method without any surfactants.

2. Experimental

$Ba_{1-x}Sr_xTiO_3$ samples with $x = 0$, 0.3, 0.5, 0.7, and 1 were synthesized by the hydrothermal method. All the chemicals were analytical grade purity. Titanium was added in the form of the precipitated hydroxide (denoted as TOH). Based on the nominal composition of $Ba_{1-x}Sr_xTiO_3$, appropriate amounts of $Ti(SO_4)_2$ were dissolved in diluted HNO_3 to form aqueous solution. Subsequently, the TOH suspension was prepared by introducing the solution into a KOH solution under stirring. To eliminate SO_4^{2-} and NO_3^- ions, the TOH precipitation was filtered and washed with distilled water for six times. Next, the fresh TOH precipitate and appropriate amounts of $Ba(NO_3)_2$ and $Sr(NO_3)_2$ solution were transferred into the stainless-steel autoclave with KOH solution for the hydrothermal treatment. The KOH concentration was adjusted to 0.1 M. The autoclave was sealed, heated up to 200 °C and held for 6 h, and then cooled to room temperature naturally. The products were filtered, washed with diluted HCl, distilled water, and absolute ethanol for several times, and then dried at 70 °C for 4 h for characterization.

X-ray diffraction was performed on a Rigaku X-ray diffractometer with high-intensity CuKα radiation. Transmission electron microscope (TEM) images were taken with a JEM-200CX TEM by using an acceleration voltage of 160 kV. Elemental analysis were carried out on a JEOL 2010 (operated at 200 kV), equipped with an energy-dispersive X-ray spectroscopy (EDX).

3. Results and discussion

The XRD patterns of the as-prepared $Ba_{1-x}Sr_xTiO_3$ (BSTO) powders with $x = 0$, 0.3, 0.5, 0.7, and 1 are depicted in Fig. 1. As shown in Fig. 1a, the strong and sharp peaks suggest that BSTO crystals are highly crystalline. All BSTO samples are of the perovskite structure due to the absence of the peak (2 0 0) splitting and that the peaks are in good agreement with those obtained from the conventional

* Corresponding author. Tel.: +86 379 65928196; fax: +86 379 65928196.
E-mail address: wangyg968@yahoo.com.cn (Y. Wang).

0925-8388/$ – see front matter © 2010 Elsevier B.V. All rights reserved.
doi:10.1016/j.jallcom.2010.03.196

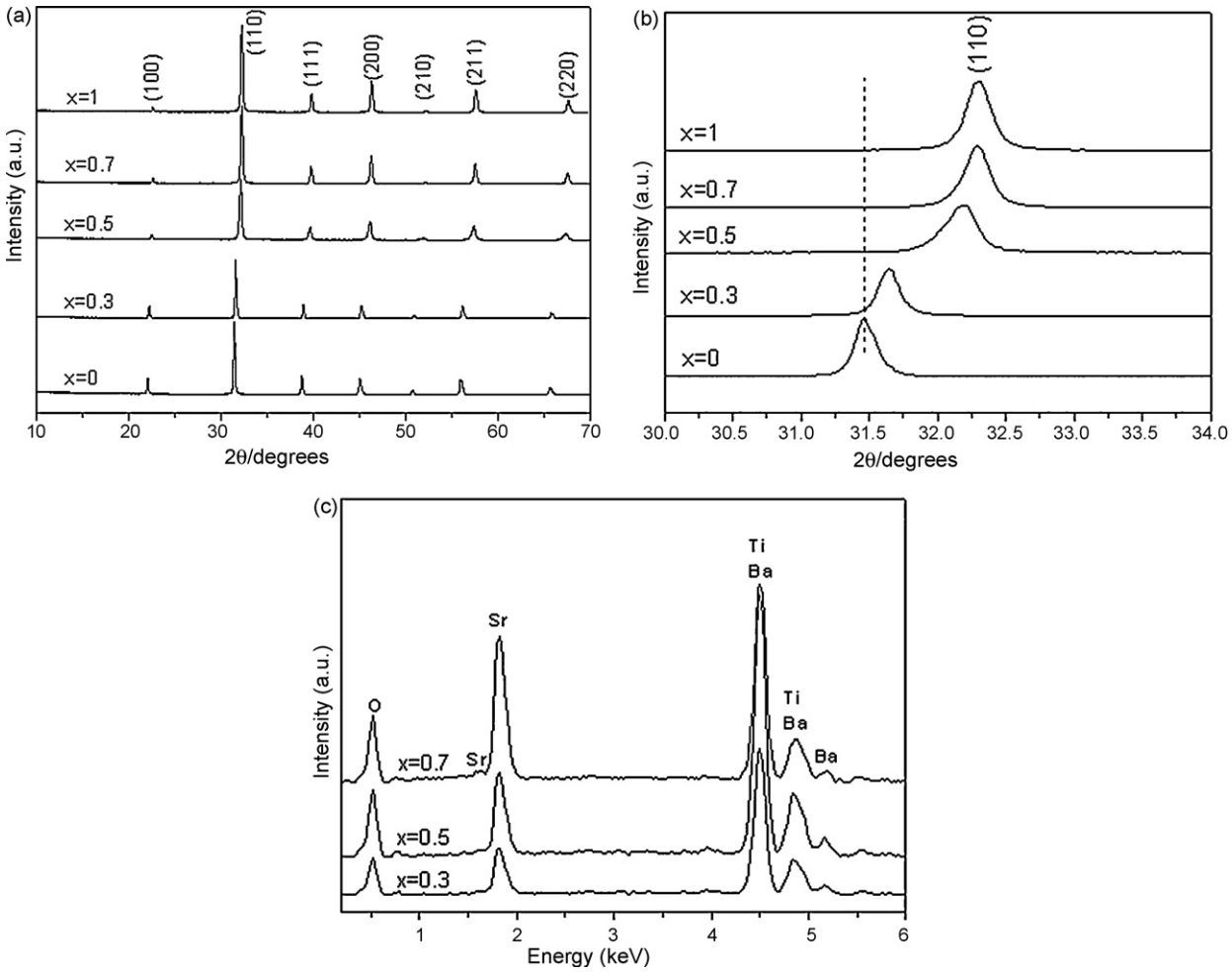

Fig. 1. (a) XRD patterns of the as-prepared $Ba_{1-x}Sr_xTiO_3$ with different values of x (x = 0–1). (b) A comparison of (1 1 0) diffraction peak positions for the patterns. (c) The EDX pattern of the as-prepared $Ba_{1-x}Sr_xTiO_3$ (x = 0.3, 0.5, and 0.7, respectively).

calcined method [25]. It is notable that the reflections corresponding to TiO_2 and (Ba, Sr)CO_3 are absent, suggesting that all the BSTO samples are of single-phase solid solution nature, regardless of the Sr/(Sr + Ba) mole ratio in samples. In fact, when x is 0 or 1, the peaks can be indexed to the cubic lattice of $BaTiO_3$ (JCPDS: 31-0174) and $SrTiO_3$ (JCPDS No.35-0734), respectively. Additionally, the reduction in the intensity values for the peak (1 0 0) is similar to the reports [14,19], which is due to the difference in atomic numbers between Ba and Sr.

Fig. 1b exhibits the XRD peaks at 2θ value between 30° and 34° for all five samples. According to Bragg equation $2d \sin\theta = n\lambda$, smaller crystal plane spacing corresponds to higher diffraction angle. It is clear that the peak shifts towards the high angle compared with that of pure $BaTiO_3$ (x = 0), which implies that the substitution of the larger Ba^{2+} ions with the smaller Sr^{2+} ions has taken place. Hence, the patterns shown in the main XRD are for single-phase cubic BSTO only [26,27]. Fig. 1c shows the EDX sketch map of the as-synthesized samples. It is evident that the intensity of the Sr signal increases notably with increasing values of x in the BSTO. Based on the above results, it can be concluded that pure $Ba_{1-x}Sr_xTiO_3$ (x = 0–1) can be synthesized by the present hydrothermal method.

Fig. 2 presents the TEM image of the as-obtained BSTO samples under the present hydrothermal condition. As shown in Fig. 2a, it is interesting to find that a vivid dendritic structure of $BaTiO_3$ crystal is obtained in the case of x = 0. The length of the trunk and the diameter of the branches of the $BaTiO_3$ dendrites are about 0.7–1.5 μm and 90–150 nm, respectively. Interestingly, when Sr proportion in the BSTO system increased from 0.3 to 1, $Ba_{1-x}Sr_xTiO_3$ dendrites were also formed and no significant changes in morphology and size can be observed. Inset in Fig. 2a, b and e is the corresponding ED pattern recorded from the entire dendritic structure, respectively, which clearly demonstrate the single-crystal nature of $Ba_{1-x}Sr_xTiO_3$ (x = 0–1) dendrites.

A detailed time course study is expected to provide direct evidence of the detailed $Ba_{1-x}Sr_xTiO_3$ (x = 0–1) dendrite formation process. In a typical process, x is kept 0 in our control experiments. As shown in Fig. 3, pure anatase TiO_2 (JCPDS 21-1272) was first formed. Furthermore, the diffraction peaks of TiO_2 became weaker and broader, and finally disappeared when the reaction time was prolonged from 15 min to 0.5 h. As the reaction time was further increased from 0.5 to 6 h, well-crystallized perovskite $BaTiO_3$ (JCPDS: 31-0174) was obtained.

Fig. 4 shows TEM images of the as-prepared samples obtained during the reaction course. At the early stages of the reaction, as displayed in Fig. 4a and b, the morphology of the obtained TiO_2 particles was spherical and the mean particle size was about 5 nm. As the reaction time was increased to 0.5 h, well-crystallized $BaTiO_3$ dendrites were formed and TiO_2 nanoparticles began to decrease (Fig. 4c). When the reaction time was further prolonged, TiO_2 nanoparticles gradually disappeared and pure $BaTiO_3$ dendrites were prepared, as depicted in Fig. 4d–g. The detailed time course of $Ba_{1-x}Sr_xTiO_3$ is similar to the above process when x varies from 0 to 1.

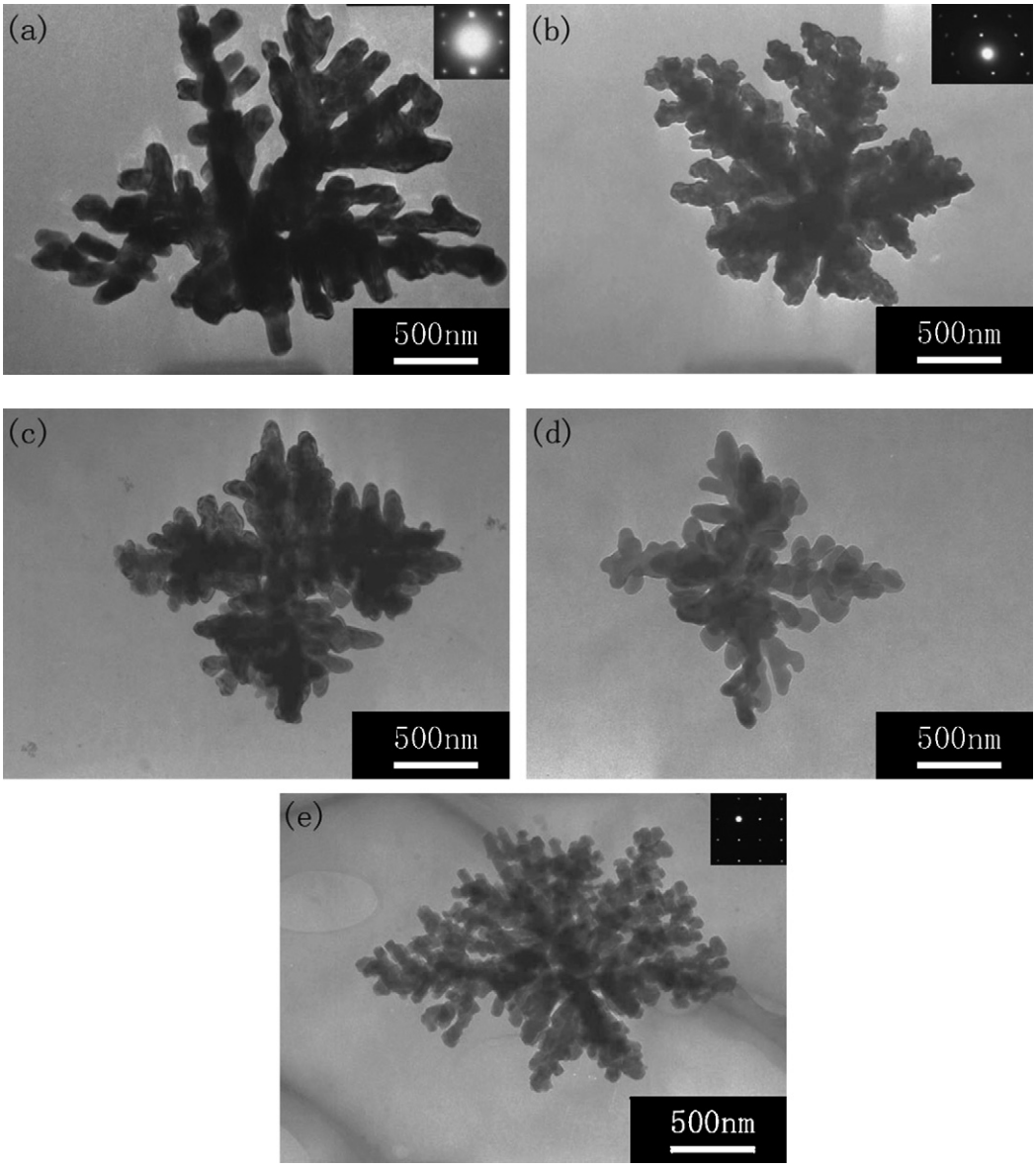

Fig. 2. TEM image of the as-prepared $Ba_{1-x}Sr_xTiO_3$ ($x = 0$–1) dendrites synthesized by the hydrothermal process at 200 °C for 6 h.

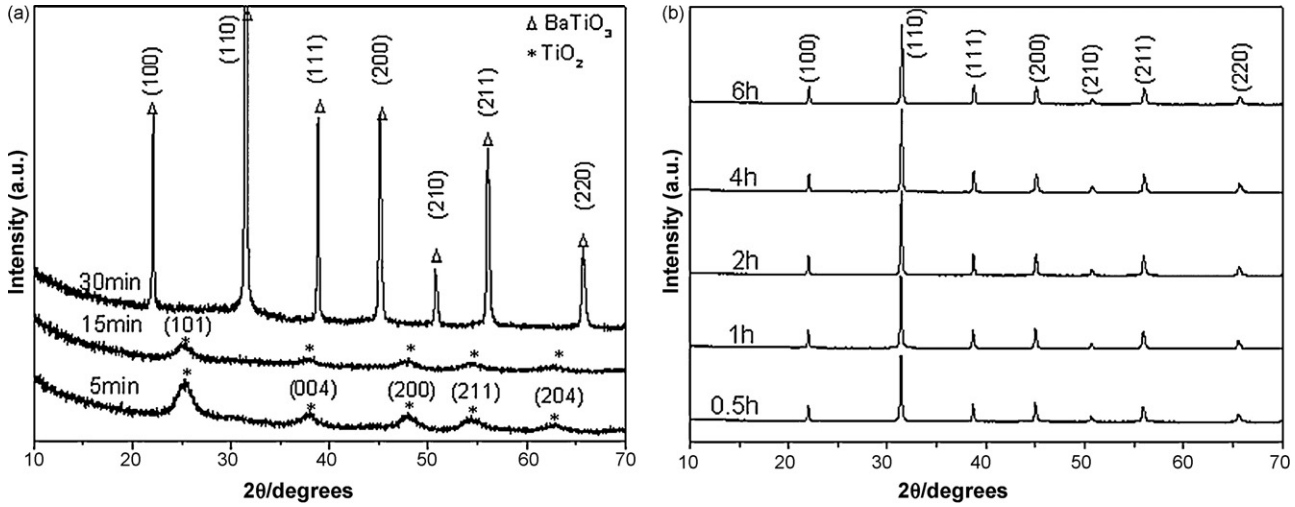

Fig. 3. XRD patterns of the as-prepared samples synthesized by the hydrothermal process at 200 °C for 5 min, 15 min, 0.5 h, 1 h, 2 h, 4 h, and 6 h, respectively.

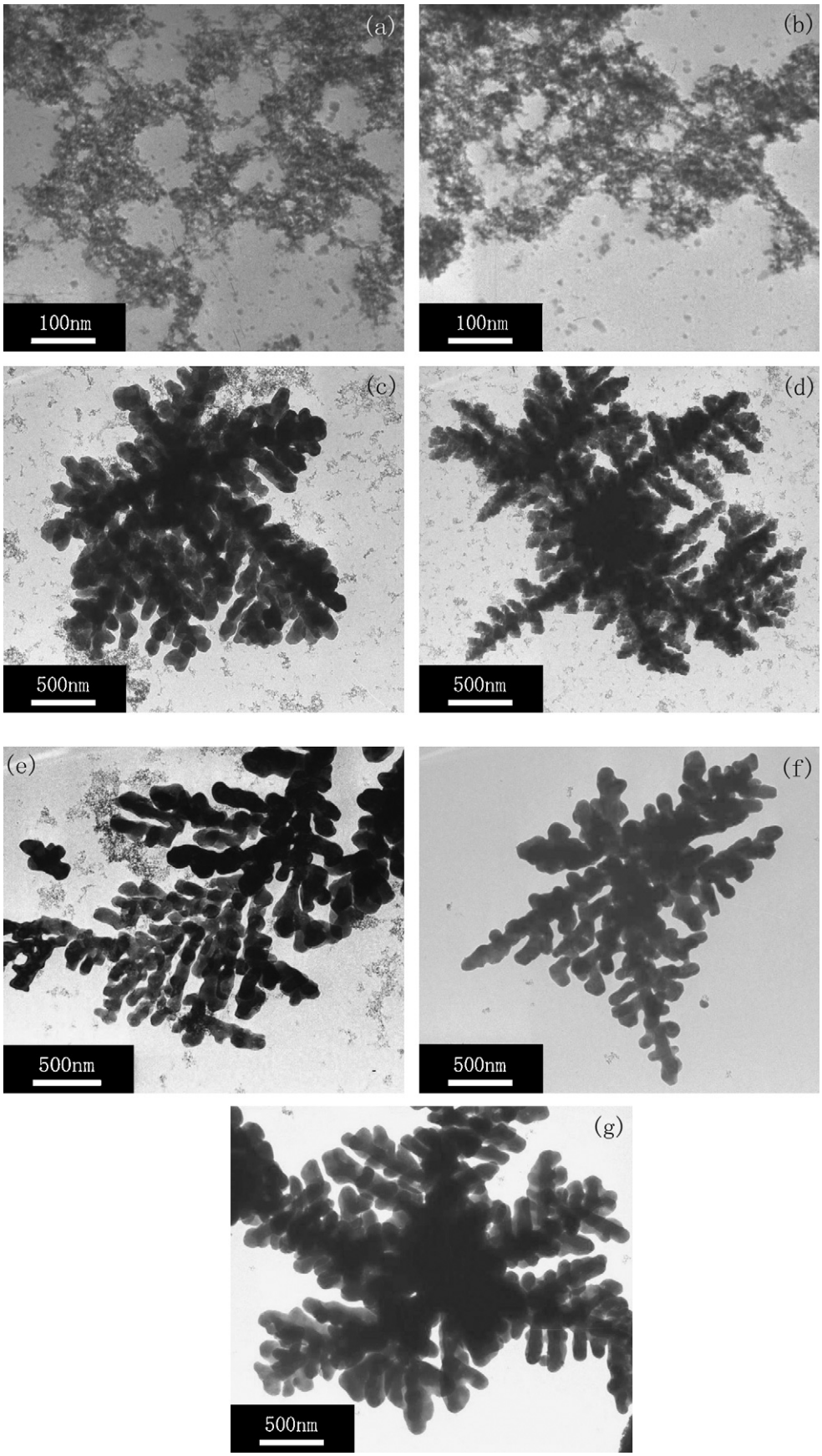

Fig. 4. TEM images of the as-prepared samples synthesized by the hydrothermal process at 200 °C for different reaction time of (a) 5 min, (b) 15 min, (c) 0.5 h, (d) 1 h, (e) 2 h, (f) 4 h, and (g) 6 h, respectively.

Based on the results of the above time course, the $Ba_{1-x}Sr_xTiO_3$ ($x = 0$–1) dendrite formation process was clear. At the early stage of the reaction, TiO_2 was first formed. Then, the reaction between solid TiO_2 nanoparticles, Ba^{2+}, and Sr^{2+} ions in solutions took place. As the reaction continued, TiO_2 nanoparticles were gradually consumed and $Ba_{1-x}Sr_xTiO_3$ crystals were formed. As the reaction mechanism and hydrothermal conditions are complicated, the exact formation mechanism for $Ba_{1-x}Sr_xTiO_3$ dendrites synthesized by the present method still needs to be further investigated.

4. Conclusions

To conclude, we report here a simple hydrothermal process for the formation of single-crystal $Ba_{1-x}Sr_xTiO_3$ ($x = 0$–1) dendrites, which may have a significant impact on the investigation of shape-dependent properties for the development of nanodevices. The $Ba_{1-x}Sr_xTiO_3$ ($x = 0$–1) dendrites formation mechanism was discussed and the synthetic process here can be extended to other perovskite oxides. Single-crystal $PbTiO_3$ dendrites have also been successfully synthesized by this simple process, which will be reported in the near future.

References

[1] X.G. Peng, L. Manna, W.D. Yang, J. Wickham, E. Scher, A. Kadavanich, A.P. Alivisatos, Nature 404 (2000) 59–61.
[2] C. Burda, X.B. Chen, R. Narayanan, M.A. Sayed, Chem. Rev. 105 (2005) 1025–1102.
[3] A. Sukhanova, A.V. Baranov, T.S. Perova, J.H.M. Cohen, I. Nabiev, Angew. Chem. Int. Ed. 45 (2006) 2048–2052.
[4] S.O. Cho, E.J. Lee, H.M. Lee, J.G. Kim, Y.J. Kim, Adv. Mater. 18 (2006) 60–65.
[5] L. Fan, R. Guo, Cryst. Growth Des. 8 (2008) 2150–2156.
[6] J. Ye, Q.W. Wang, H.P. Qi, N. Tao, Cryst. Growth. Des. 8 (2008) 2464–2468.
[7] J. Fang, H. You, P. Kong, Y. Yi, X. Song, B. Ding, Cryst. Growth Des. 7 (2007) 864–867.
[8] F. Cheng, J. Zhao, W. Song, C. Li, H. Ma, J. Chen, P. Shen, Inorg. Chem. 45 (2006) 2038–2044.
[9] Z. Chen, Z. Shan, M.S. Cao, L. Lu, S.X. Mao, Nanotechnology 15 (2004) 365–369.
[10] D. Kuang, A. Xu, Y.P. Fang, H.Q. Liu, C. Frommen, D. Fenske, Adv. Mater. 15 (2003) 1747–1750.
[11] T.M. Shaw, Z. Suo, M. Huang, E. Liniger, R.B. Laibowitz, J.D. Baniecki, Appl. Phys. Lett. 75 (1999) 2129–2131.
[12] J.H. Jeon, J. Eur. Ceram. Soc. 24 (2004) 1045–1048.
[13] Y.B. Khollam, H.S. Potdar, S.B. Deshpande, A.B. Gaikwad, Mater. Chem. Phys. 97 (2006) 295–300.
[14] D.S. Jung, S.K. Hong, J.S. Cho, Y.C. Kang, Mater. Res. Bull. 43 (2008) 1789–1799.
[15] F. Paul, J.R. Binder, H. Gesswein, H.J. Ritzhaupt, J. Hausselt, Ceram. Int. 35 (2009) 479–486.
[16] J.Q. Qi, Y. Wang, W.P. Chen, L.T. Li, H.L. Chan, J. Solid State Chem. 178 (2005) 279–284.
[17] Z. Wang, S.L. Jiang, G.X. Li, M.P. Xi, T. Li, Ceram. Int. 33 (2007) 1105–1109.
[18] M.L. Li, H. Liang, M.X. Xu, Mater. Chem. Phys. 112 (2008) 337–341.
[19] B. Hou, Y. Xu, D. Wu, Y.H. Sun, Powder Technol. 170 (2006) 26–30.
[20] B.L. Gersten, M.M. Lencka, R.E. Riman, J. Am. Ceram. Soc. 87 (2004) 2025–2032.
[21] M. Yoshimura, J. Mater. Res. 13 (1998) 796–802.
[22] L. Wang, G. Li, Z.K. Zhang, Mater. Res. Bull. 41 (2006) 842–846.
[23] J.T. Han, Y.H. Huang, W. Huang, H.B. Goodenough, J. Am. Chem. Soc. 128 (2006) 14454–14455.
[24] H.L. Wang, X.D. Ma, X.F. Qian, J. Yin, Z.K. Zhu, J. Solid State Chem. 177 (2004) 4588–4596.
[25] A. Bauger, J.C. Moutin, J.C. Niepce, J. Mater. Sci. 18 (1983) 3041–3046.
[26] Y.B. Khollam, S.B. Deshpande, H.S. Potdar, S.V. Bhoraskar, S.R. Sainkar, S.K. Date, Mater. Charact. 54 (2005) 63–74.
[27] Y.B. Khollam, S.V. Bhoraskar, S.B. Deshpande, H.S. Potdar, N.R. Pavaskar, S.R. Sainkar, Mater. Lett. 57 (2003) 1871–1879.